Feasibility of Using Neural Networks to Unfold the Response of Multi-Element TLD for Mixed Field Dosimetry

S. Y. Lee[1], J. L. Kim[2] and K. J. Lee[1]
[1]Korea Advanced Institute of Science & Technology, Yusung-gu, Kusung-dong, Taejon, Korea
[2]Korea Atomic Energy Research Institute, Yusung-gu, Dukjin-dong, Taejon, Korea

ABSTRACT

Significant advances have been made in recent years to improve calibration methodology and dose calculation algorithm in the fields of TL dosimetry. This process was accelerated in the past decade particularly in the Republic of Korea by the need to meet mandatory national accreditation requirements. The objective of this study is to develop a new algorithm to replace the simplistic decision tree algorithms by the more sophisticated neural networks in hopes of achieving a higher degree of accuracy and precision in personnel dosimetry system. The original hypothesis of this work is that the spectral information of an X and γ-ray fields may be obtained by the analysis of the response of a multi-element system. In this study, a feed forward neural network using the error back-propagation method with Bayesian optimization was designed for the response unfolding procedure. The response functions of the single element to photons were calculated by application of a computational Monte-Carlo model for an energy range from 10keV to 2MeV with different spectral proportions. The training of the artificial neural network was based on the computation of responses of a four-element system for the back-propagation method. The validation of the proposed algorithm was investigated by unfolding the 10 computed responses for arbitrary mixed gamma fields and the spectra resulting from the unfolding procedure agree well with the original spectra.

INTRODUCTION

The measurements of personal dose equivalent quantities become the determining factor force in establishing procedures, practices, and working environments that limit radiation exposure. Further, accurate measurements become the most important factor in litigation procedures. Currently, the personal dose equivalent quantities, $H_p(d)$, are determined by using multiple TLD chips with appropriate physical filters. The use of multi-element dosimeters is necessarily required of a dose assessment algorithm that weights the reading of each element for the evaluation of the dose equivalent. The optimization method using spectra found in working places are generally applied for the determination of these weights. In the past decade, a family of empirical algorithms has been developed which are based on parameterization of the response of the dosimeter to various pure and mixed fields (8). The empirical algorithms are especially effective in mixed low energy photon and beta fields and are capable of identifying the radiation field types and applying appropriate energy correction factors. These algorithms have been in routine use for several years in large-scale personnel dosimetry programs. For low doses, most common in routine personal dosimetry, empirical algorithms were recently introduced which are based on parameterization of the response of the dosimeter to various pure and mixed fields (11).

In many practical situations, one is interested not only in the dose information but also in the energy and type of radiation fields. For unknown mixed fields unfolding algorithms were developed that use numerical deconvolution techniques to identify the field components and their relative contribution (9). The response of the dosimeter is experimentally characterized in pure fields and the results are then used to create a response matrix that is applied to identify the various field components and their relative intensity in an unknown mixed field. Until now, therefore, the detection and evaluation method was carried out in a two-step procedure, first performing the measurements and in a later step the interactive unfolding of the readings of the multi-element system. Such unfolding techniques become ineffective at low dose levels where the radiation field may be identified incorrectly or the unfolding algorithm may fail to converge due to increase in the random error of the dosimeter response.

Although the dose assessment approach using conventional decision tree algorithm often provides reasonable results, uncertainties may be magnified in the current TLD systems due to the random errors associated with the characteristics of radiation fields. The objective of this study is to replace the simplistic decision tree algorithms by the more sophisticated neural networks in hopes of achieving a higher degree of accuracy and precision in the TLD system. The use of multi-element filter system can result in suitable combinations providing information on the incident photon spectra if appropriate unfolding algorithms are applied. The introduction of this intermediate step for obtaining spectral information on the incident radiation has the advantage that different dose quantity can be determined, e.g. personal dose, effective dose and organ doses. This can be performed by applications on the angular distribution of the radiation relative to the exposed person. The original hypothesis of this work is that the spectral information of an X and gamma radiation fields

may be obtained by the analysis of the response of a multi-element system. Theoretically, this could be possible because a neural network uses all of the information from the elements and the network is designed to mathematically minimize the global error in a system. Nevertheless, the ANN (Artificial Neural Networks) is trained and optimized once in a process of about 5 hour on a PC of Pentium quality. Then, the trained ANN is used for the unfolding of the measured signals, which requires less than one second of computation time. Consequently, the unfolding step can be carried out immediately after the measurements of the TL light emission by the reader system. In contrast, decision tree algorithms only use a single ratio from the badge and use the ratio boundary values for changing a correction coefficient, which has been done by eye balling points on a graph historically.

In this study, a feed forward neural network using the error back-propagation method with Bayesian optimization was adapted for the response unfolding procedure. The response functions of the single element to photons were calculated by application of a computational Monte-Carlo model for an energy range from 10keV to 2MeV with different spectral proportions. The spectra collections comprise mono spectra; spectra from ANSI N13.11 X-ray (M30, M60, M100, M150 and H150), high-energy photon (^{137}Cs) and spectra from ANSI mixed gamma sources (1). The training of the artificial neural network was based on the computation of responses of a four-element system for the back-propagation method. The validation was performed by unfolding the 10 computed responses for arbitrary mixed gamma fields. It was found that the energy spectrum resulting from the unfolding procedures agree well with the original spectrum used for the response computation.

MATERIALS AND METHODS

Determination of the element response

The design of a multi-element badge system presented here will allow beta and gamma discrimination at the various energies presents in a mixed radiation field. For this preliminary study, we use single crystals of α-Al_2O_3:C, 5mm in diameter and 1mm thick, supplied by Harshaw Bicron Co. in the form of TLD-500. As the methods for growing the crystal (i.e. α-modification) is not known exactly, the material composition data for response calculation is taken from the previous study of nominal Al_2O_3:C (12). However, as an examination of impurity shows that two types of crystal have a similar chemical composition of impurities, whatever the method used to grow the crystals, their carbon concentration is less than 0.1% by weight (6). Therefore, at concentration lower than 0.1% weight carbon is not a dominating impurity in the crystals and it will not effects on the radiation transport calculation. The principal feature of Al_2O_3:C detectors is their non-tissue equivalence, their effective atomic number being Z_{eff} = 10.2 (for tissue Z_{eff} = 7.4). This leads to the detector sensitivity dependence on photon radiation energy. The TL response to photons with energy 30keV is 2.9 times higher than the detector response to irradiation with energy 1.33 MeV (^{60}Co) as seen in Figure 1. The Al_2O_3:C TLD badge system, therefore, requires the use of special filtration since Al_2O_3:C, while more sensitive than other TLD materials, over-responds to ionizing radiations at low energy when compared with the response of tissue. That is why, to make the dosimeter sensitivity independent of photon energy, it is necessary to use correcting filters described as

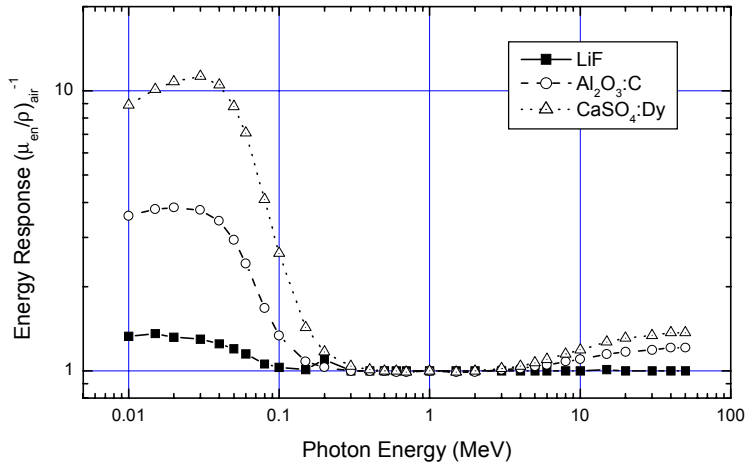

Figure 1. Energy response of the calculated kerma in luminescent materials as a function of photon energy.

followings.

Because of the small filter thickness needed and the fact that it should consider the badge response to high-energy radiations, radiation transport theory should be used to solve for the energy depositions of different radiations in the TL material. Since the analytic calculation of the energy attenuation by the materials is almost impossible except for very special cases, computer code is used to model the badge system and the radiation sources, which can be made of single or multiple energies and radiation types. The procedure used was the Monte Carlo simulation of particle transport in the filter system with the phantom within the framework of the kerma approximation. This allows testing the effect of each of the design variables on the overall badge responses. These variables include filter material for each area, filter geometry in the energy compensation area. In this study, the preliminary selection of filter material was made using the concepts of HVL (Half Value Layer) based on the mass attenuation coefficients μ/ρ (cm^2/g). Using this HVL values, the response of the Al_2O_3:C TL material to different gamma energy was found for different filter materials. After selecting the filter material combination, the design was tested against the other variables using a three dimensional Monte Carlo particle transport code called MCNP-4A (10). The phantom was assumed a homogeneous PMMA slab with a density of 1.19 $g.cm^{-3}$ each with a front face area of 30cm × 30cm and a thickness of 15cm. The following irradiation geometry was considered in the MCNP calculation. First, the dosimeter mounted on the phantom was surrounded by a vacuum and secondly, it was irradiated by a unidirectional extended photon or electron beam, the direction of which was parallel to the bottom surface of the slab and intersected the principal slab axis at a planar angle α.

The principal dosimetric region of the designed badge has four areas, three filtered and one open window. Due to the manner in which gamma attenuation coefficients change with energy, it is difficult to find out a single material or combination of practical materials have an attenuation profile as a function of photon energy that will provide the desired compensation of the energy over-response of Al_2O_3:C. It has been observed that in flattening one portion of the energy response curve, other portions will show unacceptably higher or lower energy responses. Use of three filtered regions will allow energy and radiation discrimination in the badge. The MCNP code is used to determine a measure of the relative change in the simulated TLD readout of each dosimeter area when other design variables are introduced. This is achieved by calibrating the MCNP code estimates of the open window area readout again the experimental readout of the bare TL crystal for ^{137}Cs gamma energy (662keV). The calibrated MCNP results are then used in subsequent MCNP calculations that model other areas of the badge. Each of the choices of filter materials in this study is a result of numerous MCNP calculations and of several experimental tests used to confirm the simulation results.

An auxiliary design goal in primary dosimetric area is that the filters used should be able to eliminate the presence of beta radiation in the case of mixed beta-gamma radiation exposure. Beta radiation will contribute to the readout in this area if the filter used includes a hole, and the presence of beta radiation will complicate the gamma readout giving rise to an error in the ratio $A3/H_p(10)$. A beta filter, therefore, behind the metal filter is utilized to eliminate any effects due to betas. The resultant design includes copper with a 0.06cm thickness,

Table 1. Configuration of proposed multi-element filter system.

Area	Filter material	Thickness of filter (mg/cm^2)	Total thickness (mg/cm^2)
A1	Mylar	2.8	14
	Polypropylene	9	
	Polyethylene	2.2	
A2	Polycarbonate	120	1163
	Polyethylene	154	
	Teflon	880	
	Polypropylene	9	
A3	Polycarbonate	120	997
	Polyethylene	154	
	Copper	538	
	Aluminum	176	
	Polypropylene	9	
A4	Polycarbonate	120	1001
	Polyethylene	77	
	Lead	795	
	Polypropylene	9	

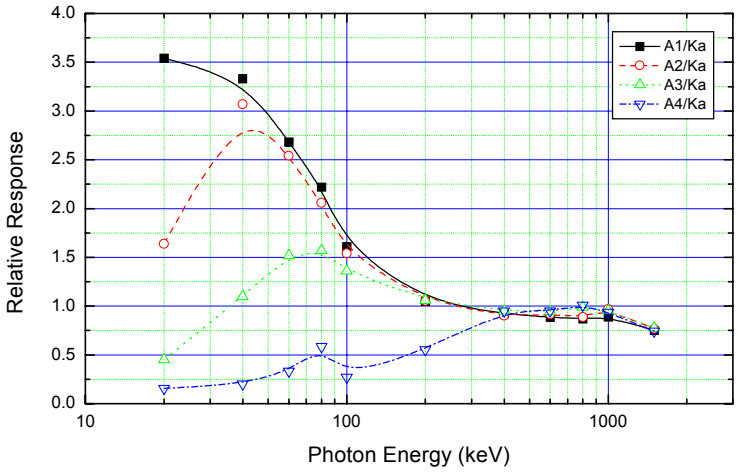

Figure 2. Relative response of the sensitive area per unit exposure as a function of photon energy.

followed by 0.65cm aluminum. The effect of this filter combination on the energy readout of Al_2O_3:C, expressed as A3/K_a, is shown in Figure 2 compared with the open window area readout, expressed as A1/K_a. It also should be noted that ratio A3/$H_p(10)$ has ranging between 0.82 and 1.1 at the effective photon energy ranges from 20keV to 1MeV as shown in Figure 3. This is within the ±30% design limits required by the ISO standard (3, 4). In case of the photon energy of 10keV, however, the ratio decreases to 0.5 %, falling outside the design limits. Therefore, this filter combination allows effect reading of the dose equivalent $H_p(10)$ received within ±20% just for energies of 20 keV or higher. A filter configuration is summarized in Table 1 and the detailed design of the badge system is discussed in another reference (5).

Analyzing the multi-element response by ANNEquation Section (Next)

The relation between the reading (registered counts) of a detection element A_j (out of N elements) and the spectral photon fluence Φ_i can be expressed by following equation:

$$A_j = \sum_{i=1}^{m} \Phi_i R_{ij} \qquad j = 1,2,3\text{K}\ ,N \tag{1}$$

where, R_{ij} represents the response per unit fluence by discrete values for the element j in the energy bin E_I and m represents the number of energy bins. The unfolding procedure aims at the solution of equation (1) for the spectrum Φ_i. One approach to solve equation (1) is the application of ANN. The basic idea of this method – applied for this purpose – is the ability of the algorithm to recognize the spectrum type from the pattern of the count vector. In the framework of ANN, the networks are trained using supervised learning, with a training set of inputs and targets in the form of $\{p_1,t_1\},\{p_2,t_2\},\text{K}\ ,\{p_n,t_n\}$. We assume that the targets are generated by $t_i = g(p_i)+\varepsilon_i$ where $g(p_i)$ is an unknown function and ε_i is independent Gaussian noise. The initial objective of the training process will be minimize the sum of squared errors:

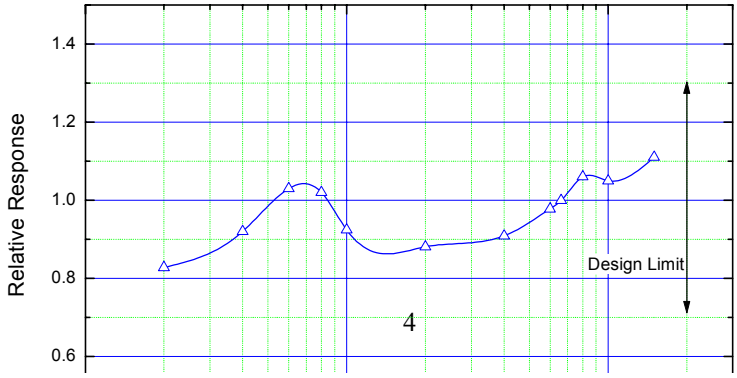

Figure 3. Relative energy response of primary dosimetric area A3 to personal dose equivalent, $H_p(10)$.

$$E_D = \sum_{i=1}^{n} (t_i - a_i)^2 \tag{2}$$

where a_i represents the neural network response.

The goal of neural network training is to produce a network, which produce small errors on the training set, but which will also respond properly to novel inputs. One of the problems that occur during neural network training is called overfitting. The error on the training set is driven to a very small value, but when new data is presented to the network the error is large. The network has memorized the training examples, but it has not learned to generalize to new situations. When a network is able to perform as well on novel inputs as on training set inputs, we say that the network generalized well. The idea is that the true underlying function is assumed to have a degree of smoothness. When the weights in a network are kept small, the network response will be smooth. With regularization, any modestly oversized network should be able to sufficiently represent the true function. Typically, training aims to reduce the sum of squared errors $F = E_D$. However, regularization adds an additional term; the objective function becomes $F = \beta E_D + \alpha E_W$, where E_W is the sum of squares of the network weights, and α and β are objective function parameter. The relative size of the objective function parameters dictates the emphasis for training. If α = β, then the training algorithm will drive the errors smaller. If α ? β, training will emphasize weight size reduction at the expense of network errors, thus producing a smoother network response. The main problem with implementing regularization is setting the correct values for the objective function parameter. It is desirable to determine the optimal regularization parameters in an automated fashion. One approach to this process is the Bayesian framework of David Mackey (7). David Mackay has done extensive work on the application of Bayes' rule to neural network training and to optimizing regularization. A detailed discussion of Bayesian regularization is beyond the scope of this paper. A detailed discussion of the use of Bayesian regularization, in combination with Levenberg-Marquardt training, can be found in other material (2).

The spectrum unfolding procedures described in this paper applies to multi-layer feed forward neural networks that are used for nonlinear regression. With the basis of the Bayesian framework, an ANN for function approximation is designed with following topology:

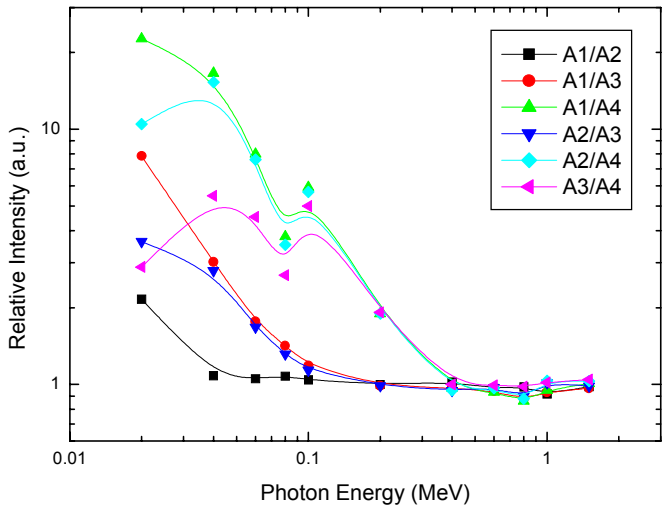

Figure 4. Schematic structure of 3-layer feed forward and back-propagation network.

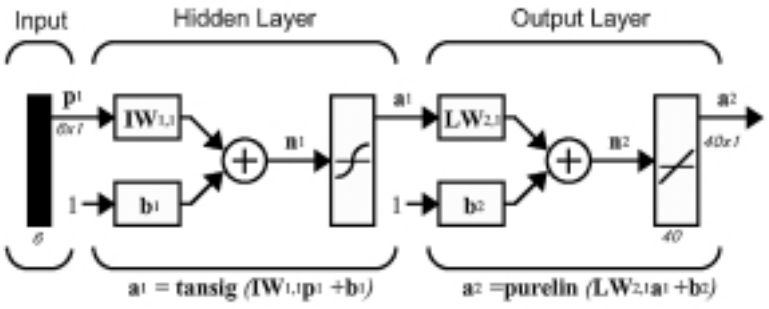

Figure 5. Response functions of a six-parameter system for ANN input vector.

Table 2. Trend of the network parameters by Bayesian optimization.

Epoch	Sum of Squared Errors (SSE)	Sum of Squared Weights (SSW)	Gradient	Number of Effective Parameter (γ)
0	2.173E+03	2.117E+02	3.620E+03	5.100E+02
50	3.650E-02	1.581E+00	3.870E-01	3.100E+02
100	2.259E-03	5.213E+00	1.190E-02	4.440E+02
150	4.378E-05	1.193E+01	1.370E-02	4.730E+02
200	5.489E-06	1.566E+01	3.990E-04	4.750E+02
250	4.711E-06	1.613E+01	3.190E-05	4.760E+02
300	4.320E-06	1.639E+01	5.770E-04	4.760E+02

- Feed forward network: There are only connections from the neurons from one layer to the neurons of the next adjacent layer; no connections across the layers are applied.
- The input layer consists of six neurons due to the six-response factor from four elements of the system.
- Two intermediate layers are used: The first intermediate layer consists of 70 neurons; the second one consists of 440 neurons.
- The output layer consists of forty neurons due to the subdivision of the gamma spectrum into 40-energy bins.
- The node transfer function is tan-sigmoid for the input neutrons and a linear function is used for the neurons from the other layers.

For the training spectra, a subset (about 5) of an overall set of 25 photon spectra − from Monte Carlo calculations − was used. A set of about 10 spectra for which it was possible to calculate the detector element responses as realistically as possible served for validation. Therefore, the selected spectra considered in this work contain at the same time gamma from 10keV to 2MeV photon energy, with different spectral proportions. The spectra collection comprises mono spectra; spectra from ANSI X-ray, photon calibration source (^{137}Cs) and spectra from ANSI mixed gamma sources (1). In order to achieve a large number of photon spectra for the training process, the primary spectra were used to create a larger set of spectra by a randomly variation of the content for single energy bins of each spectrum. In Figure 5, the element response functions are illustrated in the generalized response ratio derived from the quantity by division through the detector area. The example for thephoton spectra is also illustrated in Figure 6. The numbers of the elements in the figure are related to the detector sensitive area in Table 1.subdivision of the X-ray spectrum in 40 energy bins with respect to the optimization of the calculated dose for

RESULTS AND DISCUSSION

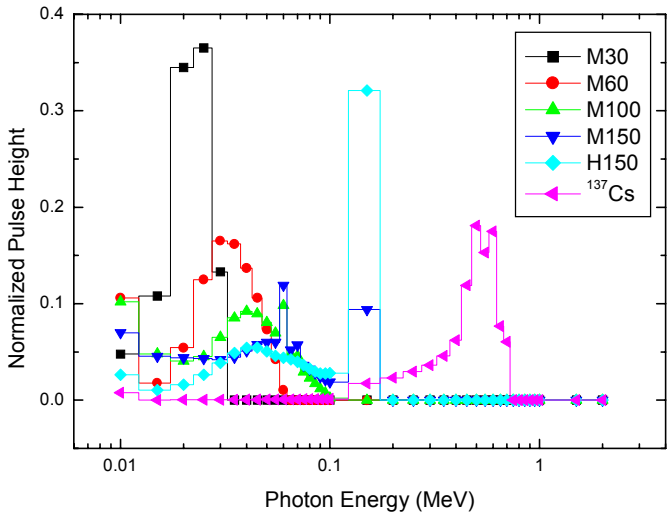

Figure 5. Example of reference spectrum for ANN target vector.

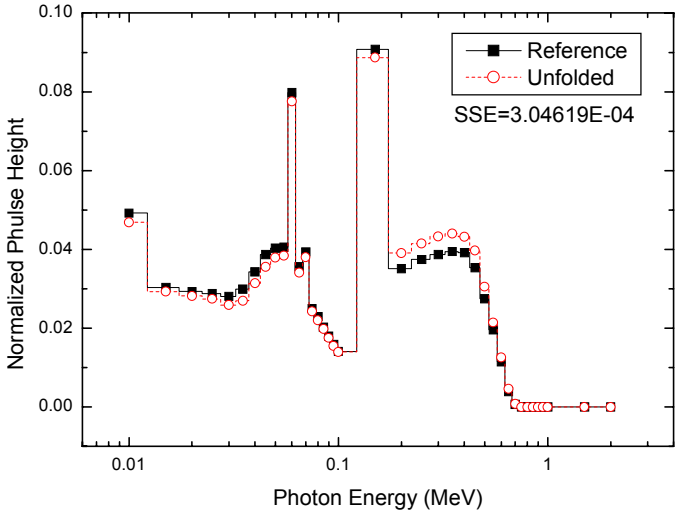

Figure 5. X-ray spectrum unfolded by ANN for ANSI M30 mixed with 20% of ^{137}Cs.

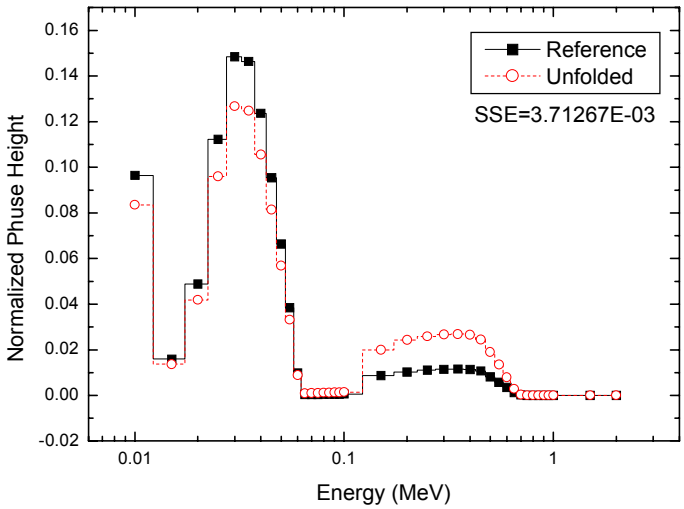

Figure 5. X-ray spectrum unfolded by ANN for ANSI M150 mixed with 70% of ^{137}Cs.

For the training of the ANN, a modified off-line back-propagation algorithm was used. The training procedure minimizes the error function, defined in this application by the sum of the square deviations of the training spectra to the spectra computed with the ANN. During the training procedure the weight constants between two neurons, which represent the strength and quality of the neuron connection (stimulating or inhibiting the output) are determined. One feature of this algorithm is that it provides a measure of how many network parameters (weights and biases) are being effectively used by the network. The back-propagation algorithm was applied in a version with momentum term, weight decay term and flat spot elimination in order to accelerate the training process. After the network training all weights of the connections are determined and the unfolding process can be derived easily from the element responses. The major difference to common optimization is that the evaluation and the optimization procedure are separated. The initial network is consisting of 6-10-40 structures, and the number of hidden neurons in hidden layer is optimized according to the network adaptation. In the process of adaptation, the network is scheduled to assess the SSE (sum of squared error), SSW (sum of squared weight) and gradient at each 50 epochs. The performance goal of the network adaptation was settled on 5.0E-6. In this study, 510 weights have to be determined, requiring on a Pentium-PC a total amount of about 5 hours. The temporal trend in the network parameters according to the network adaptation is shown in Table 2. As shown in the table, the effective number of network parameter is optimized as the epoch of the network is increased and it was found that the optimal number of the parameter is 476.

For the reconstruction of the gamma spectrum, the course of dose conversion factors with respect to the energy has to be taken into account. The corresponding calculation was performed with gamma spectra subdivided into 40-energy bins. It turned out, that the subdivision of the gamma spectra into 40-energy bins leads to dose estimates with sufficient accuracy in comparison to the spectra with full energy resolution (deviation <20%). A least square procedure was applied to find the bounds of the energy intervals for the overall energy range from 10keV to 2MeV. The typical results of spectrum unfolding of the six-parameter system that was performed by the ANN are shown in Figure 7 and 8, together with an absolute comparison with the original spectra. The comparison in both examples shows a rather good agreement between the unfolded spectrum and the original one. Therefore, it can be stated from the evaluation of 10 validation spectra, that the proposed method based on a multi-element detector in combination with the unfolding using ANN is a promising approach for the application in personnel dosimetry.

After the computed responses were unfolded, the obtained spectra were used for personal dose calculations. In this work, the unfolded spectra were folded with the dose conversion factor $Hp(10)/K_a$ and the dose value $H_p(10)$ was computed. The results of validation test are given in Table 3 and it can be found easily that the determined dose values are reproduced within accuracy better than 80%. However, it also turned out that, in a photon energy range from 20keV to 100keV, the dose values for computed mono-energetic photon spectra might be overestimated by a factor of two. The reason is the similarity of the element response functions in this energy range what results in a limited energy resolution of the incident photons. One limitation in comparison to conventional methods is, that a change in the resolution of the photon spectrum, i.e. a change of energy bins in number or bounds, requires also a change of the ANN topology and a new training procedure must be performed. In conventional procedures, changes in the energy resolution can be carried out at the beginning of each unfolding process.

CONCLUSION AND FURTHER SUTDY

In this feasibility study, we were try to propose the new dose assessment algorithm for multi-element TLD system to replace the simplistic decision tree algorithms by the more sophisticated neural networks in hopes of achieving a higher degree of accuracy and precision. We also introduced the Bayesian algorithm to optimize the general MLBP (Multi-Layer Back Propagation) neural network. It was demonstrated that a multi-element dosimeter system with an unfolding algorithm based on artificial neural network is suitable to obtain spectral information on the incident photons It was also found that the Bayesian's approach was helpful to optimize the connective weights to solve the abnormal function overfitting. For the unfolding of the multi-element response, merely these weights were applied without carrying out further optimizations. In consequence, the unfolding step requires less than one second, i.e. several orders of magnitude less of computational time in comparison to the optimization step. Therefore, the response unfolding can be carried out frequently and can be implemented either as hardware or as software into the measuring instrument in this topology. Although the theoretical feasibility of the method was only demonstrated in some examples, further important subjects for future study will be to investigate the validation of the method by experiments, and compare the unfolding techniques with common unfolding methods.

Table 3. Example of personal dose assessment by ANN spectrum unfolding algorithm.

Test Category	HEP (^{137}Cs)	SSE	$H_P(10)$ (Sv)			$H_P(0.07)$ (Sv)		
			Delivered	Calculated	Relative error	Delivered	Calculated	Relative error
M30	20%	7.034E-04	1.521E-15	1.277E-15	1.604E-01	3.703E-15	2.045E-15	4.479E-01
M60	70%	3.564E-05	1.923E-15	1.767E-15	8.096E-02	2.306E-15	2.641E-15	1.454E-01
M100	20%	1.375E-02	1.760E-15	1.559E-15	1.139E-01	1.728E-15	2.594E-15	5.012E-01
M150	70%	1.907E-04	1.965E-15	1.833E-15	6.714E-02	1.823E-15	2.330E-15	2.779E-01
H150	20%	2.020E-04	2.082E-15	2.043E-15	1.878E-02	1.911E-15	2.268E-15	1.870E-01
^{137}Cs	100%	1.035E-05	6.673E-15	6.807E-15	2.020E-02	6.618E-15	6.960E-15	5.162E-02

REFERENCES

1. ANSI, American National Standard for Dosimetry-Personnel Dosimetry Performance-Criteria for Testing. ANSI/N13.11, American National Standards Institute, Inc. (1993).
2. F.D. Foresee and M.T. Hagan, Gauss-Newton Approximation to Bayesian Regularization. The 1997 International Joint Conference on Neural Networks, 1930-1935 (1997).
3. ISO, Personal and Environmental Thermoluminescence Dosimeters. ISO Standards DP 8034, ISO/TC85/SC2/WG7 (1984).
4. ISO, Criteria and Performance Limits for the Periodic Evaluation of Processors of Personal Dosemeters for X and Gamma Radiation. ISO/PRF 14146 (1997).
5. S.-Y. Lee and K.J. Lee, Development of Personal OSL Dosimeter for Mixed Radiation Fields Based on α–Al_2O_3:C. Radiat. Prot. Dosim., in press (2000).
6. S.-Y. Lee and K.J. Lee, Optical Responses of α-Al_2O_3:C by Multi-Wavelength Stimulation for Mixed Field Dosimetry. The 9th International Conference on Radiation Shielding, Tsukuba, Japan (1999).
7. D.J.C. Mackey, Bayesian Interpolation. Neural Computation. 4, 415-447 (1992).
8. M. Moscovitch, Dose Algorithms for Personal Thermoluminescence Dosimetry. Radiat. Prot. Dosim. 47(1/4), 373-380 (1993).
9. M. Moscovitch, J.D. Chamberlain and K.J. Velbeck, Dose Determination Algorithms for a Nearly Tissue Equivalent Multi-element Thermoluminescent Dosimeter. TM-10971, ORNL, Orlando (1988).
10. ORNL, MCNP4A:Monte Carlo N-Particle Transport Code System. CCC-200, ORNL (1993).
11. I.M. Rayes and T.G. Stoebe, Personnel Dosimetry Badge System for Mixed Radiation Fields Based on Teflon-Embedded $CaSO_4$:Dy TLD Material. Radiat. Prot. Dosim. 32(1), 5-13 (1990).
12. I. Tale, et al., Optical Properties of Complex Anion Vacancy Centers and Photo-Excited Electronic Processes in Anion Defective α-Al_2O_3:C. Radiat. Prot. Dosim. 65(1-4), 235-238 (1996).